Research Article – Vol. 02, Issue 02, No. 07

Advanced in Engineering and Intelligence Systems

Journal Web Page: https://aeis.bilijipub.com

Four Central Nanocavity of Ultra-Sensitive Refractive Index Biosensor for Cancer Detection in Hexagonal Photonic Crystal

William Matsui[1,*] , Jianqiao Fang[2]

[1] Dell Medical School, the University of Texas at Austin, Austin, Texas

[2] Zhejiang Chinese Medical University, Hangzhou Zhejiang 310053, China

Highlights

- *Novel biosensor design using four center nanocavities in a hexagonal photonic crystal.*
- *Biosensor capable of detecting cancer cells from normal cells based on refractive index changes.*
- *Resonant wavelengths in the range of 1.491258μm to 1.50588μm enable cancer cell detection.*
- *Low power loss (<2%) and short delay time (2ps) in the proposed biosensor structure.*
- *High sensitivity, quality factor, and Figure of Merit surpassing similar structures in speed and sensitivity.*

Article Info

Received: 18 April 2023
Received in revised: 28 May 2023
Accepted: 28 May 2023
Available online: 29 June 2023

Keywords

Photonic Crystal,
Optical Biosensor,
Cavity-Coupled Waveguide,
High Sensitivity

Abstract

We design and analysis of a novel biosensor with four center nanocavity in hexagonal photonic crystal (PhC) is presented. This biosensor can detect cancer cells from normal cells. The main performance of the detection is based on glass nanocavity and the samples refractive index. In proposed biosensor, four central nanocavities are immersed in the samples and the resonant wavelengths change according to the refractive index. The resonant wavelengths range for the detection of cancer cells is λ0=1.491258μm ~ 1.50588μm. The power loss in the proposed structure is less than 2%, and the delay time is 2ps. At best, the sensitivity and quality factor parameters are 734nm/RIU and Q.f=2330.09, respectively. The Figure of Merit (FOM) or detection limit is 412.87±45.87RIU-1. The biosensor footprint and the design method are 102.6μm2 and FDTD, respectively. Proposed device is a higher speed and sensitivity in detection samples than similar structures.

1. Introduction

Two-dimensional photonic crystals (2D-PhC) are used in the proposed device, From dielectric cylinders that are placed at equal distances and in a hexagonal grid. [1]. One of the major advantages of two-dimensional photonic crystals is their photonic bandgap (PBG) or Forbidden frequency. When the refractive index of dielectric or cylindrical rods differs from the refractive index of the area (here it is air), a photonic bandgap is formed [2]. This important advantage is used to control the light in the structure, which means that the photonic bandgap allows us to direct and control the light signal in any direction it needs. [3]. To design a structure, a waveguide is created by removing several dielectric rods, which is called a linear defect. Or you can add a rod with different material or radii, which is called a point defect. Create one in these crystals. Due to the high flexibility of photonic crystal it can operate in different applications. A few examples of different applications include biosensors [4], fibers [5], analogue to digital converters [6,7], accelerometers [8], logic gate [9,10]. Optical sensors have special advantages over electronic sensors, such as no noise, much faster, easier maintenance, and no use of dangerous electronic components that can sometimes explode. Optical sensors, on the other hand, have much lower sensitivity and error detection than electronic sensors. The best methods used for optical sensing based on annular intensifiers are photonic crystals and surface plasmon technology, color resonant, and interferometric methods [11,12]. Biosensor sensing indicates the ability to detect changes in the

* Corresponding Author: Augustinus Sieck
Email: william.matsui@utexas.edu

physical properties of the samples. Biosensors have many applications, including the detection of cancer cells, diabetes cells, cells, food analysis, DNA classification, microbial sensors, and glucose monitoring [3]. Therefore, biosensors have attracted the interest of many researchers around the world. Recently, the Photonic Crystal Biosensor (PhC) has received much attention due to its simplicity and high sensitivity [13]. One of the most common ways to diagnose diabetes is to take a blood sample from a patient, which is called an invasive procedure. This includes the concentration of glucose in the blood, plasma, or serum samples, which is done by pinpricking. [14]. Another way is to use "test strips". In this method, due to airborne dust or the interference of fingerprints with the tape and other events, the detection error in this method increases. Fluorescent signal detection methods cannot operate without a label and require expensive photon detection equipment to use this method [15-18]. The sensitivity of SPRs is strongly affected by the quality (thickness, roughness, and evenness) of the deposited metal and, unless modified by a specific enzyme, they cannot measure complex compounds [19,21]. With high blood sugar, a person can develop diabetes. This happens when the body does not produce enough insulin and the other cells do not respond to the insulin injection. Complications that occur in people with diabetes can be repeated urination, and hunger, thirst.

Much work has been suggested in this area to try to improve the structure. Based on studies and work done, we concluded that the main problems and challenges in biosensor structures are sensitivity, quality factor, and power loss. The structure of the all-optical biosensor based on the ring resonator was proposed by Mr. Chopra et al. This structure can detect cancer and diabetes. The sensitivity of this structure is S=6.567nm/RIU and the quality factor is at best Q.f=1011.48 [22]. In year 2019, Mr. Rajendran et. proposed structural that at best transmission power is 98% and have a quality factor of 267. [23]. This article consists of five main sections, the first of which introduces photonic crystals biosensors and describes the samples to be detected. The second part of the mathematical theory and the way light interacts with matter is investigated through Maxwell equations. The third part of the proposed structure is introduced along with the design specifications and dimensions. The fourth section discusses the simulation results and structure outputs and finally concludes in the five section. Due to the immersion of central nanocavities in the samples, we will have an accurate detection and a high speed due to its small size.

2. Numerical Method

This paper aims to measure and detect cancers cells using two-dimensional photonic crystals. To study the electric field efficiently, the photonic crystal structure is used by analyzing the electric field distribution and the amplified wavelength using the plane wave propagation (PWE) technique. The Maxwell equations used by dielectric materials to control the propagation of electromagnetic waves are as follows:

$$\nabla.H = J + j\omega D \tag{1}$$

$$\nabla.E = -j\omega B \tag{2}$$

$$\nabla.B = 0 \tag{3}$$

$$\nabla.D = \rho \tag{4}$$

Where E, H, D, B, ρ, and J represent the electric field, magnetic field, electric displacement field, magnetic induction field, free charge density, and free current density, respectively. Equations (1) and (2) are field gradients. Equations (3) and (4) diverge in the field vector. If it is assumed that there is no free charge and current, the Maxwell equations can be solved, which gives the Helmholtz equation for the propagation of the electric field distribution in photon crystals [24], therefore:

$$E(r) = E_{k.r}(r) \times e^{i.k.r} \tag{5}$$

In the following equation, $E_{k.r}$ shows the electric field as a function of the square grid rotation. Finally, the expression for the distribution of the electric field can be obtained in the form of a Bloch wave, which in terms of the Fourier series extends throughout the network vector such that:

$$E_{k.r}(x,y) = \sum E_{k.r}(G_r) e^{(i.(kx+G_{x.r}).x+(ky+G_{y.r}).y)} \tag{6}$$

Given the high importance of the sensitivity parameter in all-optical biosensors, the sensitivity value is calculated from the following equation.

$$S_\lambda(\frac{nm}{RIU}) = \frac{\Delta\lambda_p}{\Delta n} \tag{7}$$

Where $\Delta\lambda_P$ is the difference between the changes in the resonance wavelength, and Δn is the difference in the refractive index related to the same wavelengths.

Another important parameter is the proposed sensor resolution, which is considered as a key parameter for the ability to perform sensor performance, which is high accuracy with a slight change in refractive index.

$$R(RIU) = \Delta n_a \times \frac{\Delta\lambda_{\min}}{\Delta\lambda_{peak}} \tag{8}$$

Also, another important factor in detecting an optical sensor is the quality factor parameter of the structure, this parameter has a direct relationship with

the sensitivity parameter. The quality coefficient can be calculated from Equation (9), [45].

$$Q.f = \frac{\lambda_d}{\lambda_{FWHM}} \quad (9)$$

In Eq. (9), λ_d represents the resonant wavelength of the central dielectric rods, and λ_{FWHM} represents the full wavelength of half of the reflected signal wavelength.

3. Photonic Bandgap and Optical Biosensor

The proposed device is designed in a two-dimensional photonic crystal bed, and the dielectric rods, which are made of silicon, are formed in the air. The silicon dielectric rods of radius r=0.2a are forming hexagonal with a lattice index a=600nm. The dielectric constant of the silicon dielectric rods is equal to 3.42 at wavelength 1200nm. After plane-wave expansion (PWE) simulation, this structure is found to possess a TM photonic bandgap in the frequency range of ω_1 € [0.2655,0.4352] with $\Delta\omega_1$=0.1697 and ω_2 € [0.5435,0.5826] with $\Delta\omega_1$=0.0391, as shown in Fig. 1(a). Given that the frequency range of the ω_1 is larger than the ω_2, the bandgap TM is used as the working range in the proposed structure. According to the calculations of the bandgap frequencies in the TM and TE polarization modes, the wavelength of the proposed structure is between λ=1378nm ~ 2259nm. Fig. 1 (b) shows the transmission of the optical signal through the central wavelength of 1.55μm in the polarization state of TM and TE.

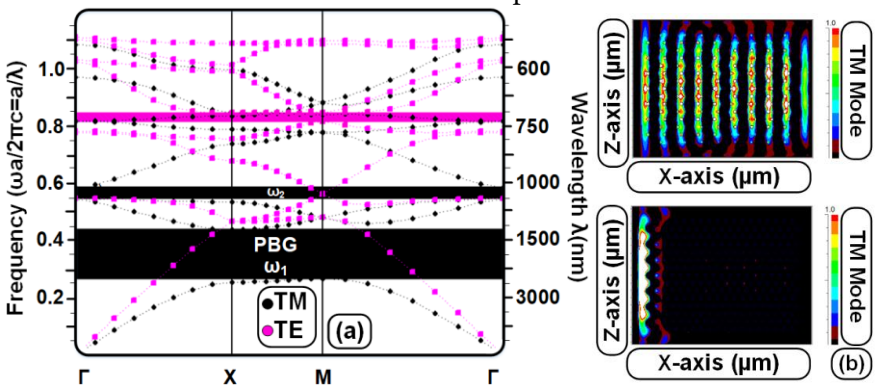

Fig. 1. (a) The Photonic bandgap, (b) Spectrum transmission.

The proposed biosensor structure is based on hexagonal two-dimensional crystal photonics. The wavelength selection is performed by the coupled ring resonator to the input and output waveguides. The pink dielectric rod near the ring resonator is used to increase the quality factor of the output signal and its distance to the center of the green rod is equal to 300 nm. Four central nanocavity techniques were used to sense the samples marked in the center of the structure in red. The distance between the center to the center of the red dielectric rods is 240 nm. The region marked in black is a cavity made of the glass wall where the samples are located. So, the green, red and pink rods float within the samples. The cavity glass wall has a refractive index of n_G=1.5, which is added when calculating the refractive index of the specimens poured into the glass cylinder.

$$n_t = n_G + n_S \quad (10)$$

where n_t is total refractive index used to calculate the important parameters in the output, n_G is the glass refractive index and n_S is the samples refractive index. The number of silicon dielectric rods is in the x-axis 19 rods and in the y-axis is 15 rods, so the overall dimensions are equal to 102.6μm²

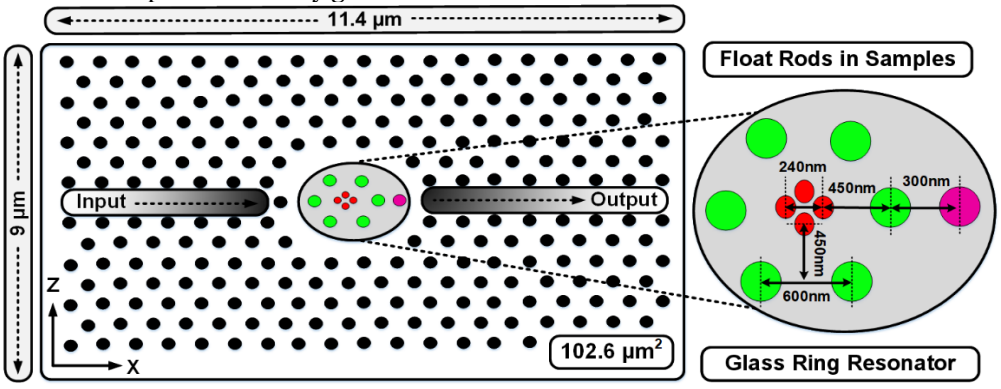

Fig. 2. The Proposed Optical Biosensor.

4. Result and Discussion

The proposed biosensor performs the detection function based on the sample refractive index. The important parameters to be considered in this section are sensitivity, figure of merit, quality factor, and transmission power. In the first step, a Gaussian pulse with a central wavelength of 1.55µm is applied to the input port, which is characterized the resonant wavelength chosen by the glass ring resonator. As can be seen in Fig. 3, the resonance wavelength chosen by the glass ring resonator without placing the sample is equal to 1.422µm. The average bandwidth of the resonant wavelength at the output is 1.4nm, so the quality factor of this signal is Q.f=1015.71nm. In this case, it transmits 99% of the input optical signal power intensity to the output of the proposed structure, so the power loss for this mode is equal to 1%.

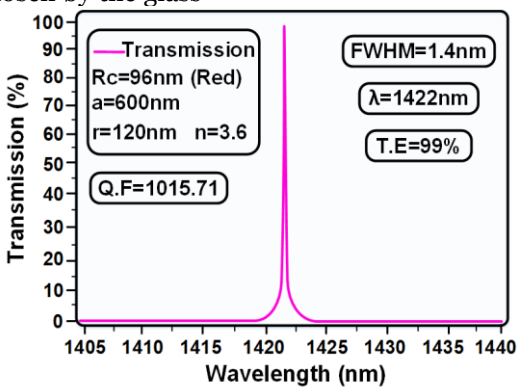

Fig. 3. The resonant wavelength without sample.

This section introduces the cancer cells refractive index to be detected by the proposed structure. Table 1 shows the refractive index of different cancer cells. As can be seen, the refractive index of the selected cancer cells is between 1.350 to 1.401, with the application of specimens with cancer cells causing the shift of the resonator wavelength at the output and detectable.

Table 1. The refractive index of the cancer cells.

Cancer Cells	RI
Normal	1.360
Culture medium	1.350
Jurkat	1.390
HeLa	1.392
PC12	1.395
MDA-MB-231	1.399
MCF-7	1.401

By placing a Culture medium cell (n_s=1.350) sample inside the structure glass resonator cavity, the glass refractive index (n_G=1.5) is added to the cancer cell refractive index, which equals n_t=2.85. The optical signal is then applied to the structure as a Gaussian pulse with a central wavelength of 1.55µm, As can be seen in Fig. 4 (a), the resonance wavelength is plotted for normal and cancerous states. The resonance wavelength for the normal sample state is 1498.54nm and for the Culture medium cancer cell sample state is equal to 1505.88 nm. When a normal person's blood sample is placed inside the proposed structure, it transmits approximately T. E=92% of the power intensity, so in this case we have an 8% power loss, and if the sample with the Culture medium cancer cell is inside the proposed structure, it transfers about T. E=91% and creates about 9% power loss. The sensitivity for the detection of the Culture medium cancer cell was S=734nm/RIU, according to which the Figure of Merit for that condition calculated FOM=412.87±45.87 RIU^{-1}. In the proposed structure, the value of the quality factor for the normal sample is calculated Q.f=936.58 and obtained to identify the cancer sample is Q.f=752.94. In Fig. 4 (b), The Jurka cell cancer is detected from the normal cell and the important parameters in the detection are calculated. The average bandwidth of the resonance wavelength for normal and cancerous samples is $FWHM_{(Norm)}$=1.6nm and $FWHM_{(Jurkat)}$=0.92nm, respectively. The sensitivity value for detecting Jurkat cancer cell is S=242.6nm/RIU. The

Form of Merit in this case is FOM=207.65±56.03RIU^{-1}. The power loss rate in this case is reduced by 2% compared to the previous state and equals 7%, so that 93% of power is transferred to the output. The resonance wavelength in this detection is $\lambda_{(Jurkat)}$=1491.262nm. The distance between the resonant wavelengths in this figure is Δλ=7.278nm. In Figure 4 (c), Hela cancer cell is detected from a normal cell with a sensitivity of S=227.46 nm/RIU. In this case, the sensitivity is reduced compared to the previous state, whereby the value of the Figure of Merit is reduced and is equal to FOM=146.91±4.738 RIU^{-1}. In the next figure (Fig 4 (d)), as the cancer cell refractive index increases, the sensitivity decreases. The PC12 cell detection has been calculated with a S=208nm/RIU of which also Figure O.f Merit is FOM=217.94±87.94RIU^{-1}. Transmission power value has increased to T. E=98%, which has the highest Transmission and lowest power losses. In Fig. 4 (e), MDA-MB-231 cell with S=186.69nm/RIU is detected. The value of the parameter of the quality factor is also equal to Q.f=2294.24. The resonant wavelength and the average bandwidth are obtained as $FWHM_{(Norm)}$=1.6nm and $FWHM_{(MDA\text{-}MB\text{-}231)}$ =0.65nm, respectively. Finally, in Fig. 4 (f), MCF-7 cell cancer is detected from the normal cell. The average bandwidth in this detection is at its best, which is equal to $FWHM_{(MCF\text{-}7)}$ =0.64 nm. Given the high detection accuracy for MCF-7 cancer cell, the value of the quality factor also reached the highest value and is equal to Q.f=2330.09. According to the obtained results, it can be concluded that in the detection of MCF-7 cancer cell from normal cell has the best accuracy and quality factor.

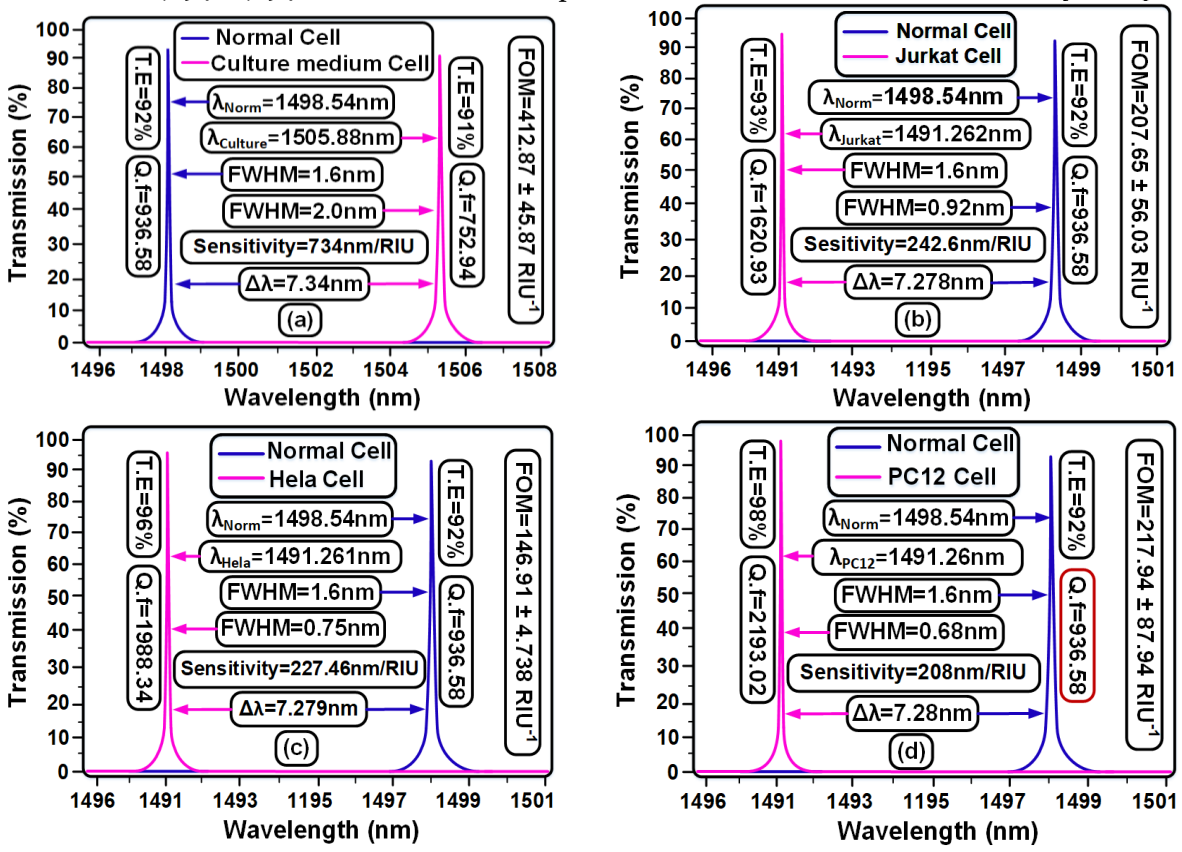

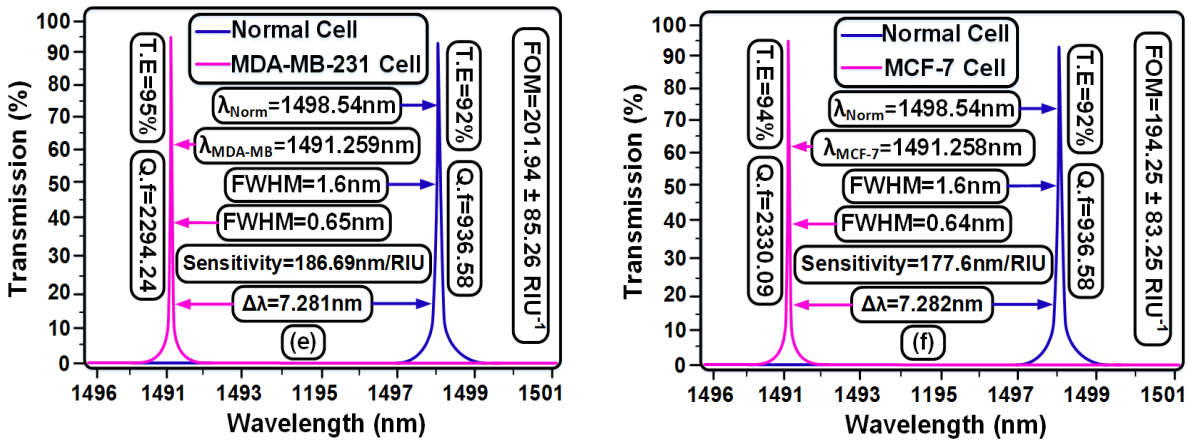

Fig. 4. The resonance wavelengths for cell cancer detection, (a) Culture medium, (b) Jurkat, (c) Hela, (d) PC12, (e) MDA-MB-231, (f) MCF-7.

In Table 2, all the important parameters in the proposed structure are calculated. As can be seen in this table, increasing the refractive index of the cancer cell samples, reduces the average bandwidth and increases the quality factor. The lowest bandwidth and the highest quality factor were obtained in the detection for normal cell from MCF-7 cancers cell. The highest sensitivity and accordingly the Figure of Merit to detection of the Culture medium cancer cells from normal cells was obtained. The percentage of transmission powers is in the range of 91% to 98%, with the highest transmission being PC12 cell cancer detection and the lowest transmission being the Culture medium cell cancer detection. The highest sensitivity and figure of merit is in the detection of Culture medium cell and the least sensitivity and figure of merit for the detection of MCF-7 cell cancer.

Table 2. Calculated of the important parameters in the proposed structure.

Samples	λ_o (nm)	$\Delta\lambda$ (nm)	Q.f	TE (%)	FOM (RIU^{-1})	S (nm/RIU)
Normal	1498.54	1.6	936.58	92	-	-
Culture medium	1505.88	2	752.94	91	412.87±45.87	734
Jurkat	1491.262	0.92	1620.93	93	207.65±56.03	242.6
Hela cell	1491.261	1.5	994.17	96	146.91±4.738	227.46
PC12	1491.260	0.68	2193.02	98	217.94±57.94	208
MDA-MB-231	1491.259	0.65	2294.24	95	201.94±85.26	186.69
MCF-7	1491.258	0.64	2330.09	94	194.25±83.25	177.6

In this section, the delay time section, or the time when the optical signal reaches its steady-state at the proposed structure, is shown in Figure 5. This delay time is best measured at PC 12 cell detection. As shown in the figure, the delay time is 2ps and the transmission percentage is 98%.

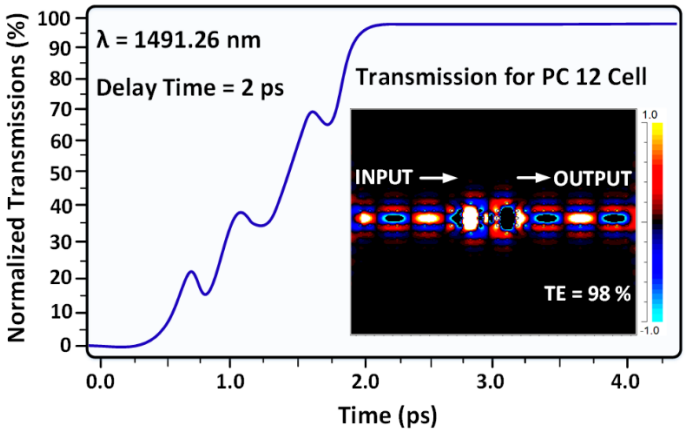

Fig. 5. Spectrum transmission.

In this section, our designed structure is compared to the structures of others. As shown in Table 3, the sensitivity has a high value and the parameters of quality factor, bandwidth and power transfer percentage have been improved compared to other structures. Table 4 shows the parameters related to the structure design.

Table 3. Comparison of important parameters of the proposed biosensor with previously reported biosensors.

Ref	App	Q.f	FOM (RIU^{-1})	TE (%)	S (nm/RIU)
Ref [25]	Blood, Tears fluid	1082	-	-	6.5764
Ref [26]	Glucose	-	-	86	422
Ref [27]	Glucose	1.11×10^5	1117	92	462
Ref [28]	Blood	262	-	100	-
Ref [29]	-	-	88	98	263
Ref [30]	-	1264	84	90	840
This work	Cancer	2330.09	412.87±45.87	98	734

Table 4. Parameters used to design and simulate the proposed biosensor.

Parameter	Symbol	Quantity	Unit
Center wavelength	λ_o	1550	**nm**
Normalized band gap (TM)	a/λ	0.2655 ~ 0.4352	**-**
Corresponding wavelength of band gap	λ	1378 ~ 2259	**nm**
Lattice constant	a	600	**nm**
Radius of rods	r	120	**nm**
Distance between the red dielectric rods	Rc	240	**nm**
Background refractive index (air)	n_{gb}	1	**-**
Linear refractive index (n_{Si})	n_o	3.42	**-**
Glass refractive index	n_G	1.5	**-**
FDTD temporal grid (time step size)	$c\Delta t$	5	**nm**

5. Conclusions

The designed sensor is able to detection of cancer cells sample from a healthy sample. In the proposed design, detection is performed by four central nanocavity resonances. Due to the importance of the accuracy and sensitivity parameter in the design of sensors, the calculation of full width at half maximum is in the best case FWHM=0.64nm and the Figure of Merit FOM=412.87±45.87RIU^{-1}. The sensitivity is at best S=734nm/RIU and the Quality factor is Q.f =2330.09. The total footprint of the structure is 102.6μm^2. The response time of the structure or the delay time in PC12 Cell is equal to 2ps. According to the output results of the simulations, the proposed biosensor, in addition to having high detection speed and small dimensions, has a high sensitivity to other similar structures.

REFERENCES

[1]Y. Zhao et al., "Review on the optimization methods of slow light in photonic crystal waveguide," IEEE Trans. Nanotechnol. 14, 407–426 (2015).

[2]C. Jamois et al., "Silicon-based two-dimensional photonic crystal waveguides," Photonics Nanostruct. Fundam. Appl. 1, 1–13 (2003).

[3]H. Dutta, A. K. Goyal, and S. Pal, "Sensitivity enhancement in photonic crystal waveguide platform for refractive index sensing applications," J. Nanophotonics 8, 083088 (2014).

[4]Sani, Mojtaba Hosseinzadeh, and Saeed Khosroabadi. "A novel design and analysis of high-sensitivity biosensor based on nano-cavity for detection of blood component, diabetes, cancer and glucose concentration. "IEEE Sensors Journal", (2020).

[5]Saghaei, H.: Dispersion-engineered microstructured optical fiber for mid-infrared supercontinuum generation. Appl. Opt. 57, 5591 (2018).

[6]Sani, M.H., Khosroabadi, S., Nasserian, M.: High performance of an all-optical two-bit analog-to-digital

converter based on Kerr effect nonlinear nanocavities. Appl. Opt. 59, 1049–1057 (2020).
[7]Sani, M.H., Khosroabadi, S., Shokouhmand, A.: A novel design for 2-bit optical analog to digital (A/D) converter based on nonlinear ring resonators in the photonic crystal structure. Opt. Commun. 458, 124760 (2020).
[8]Ahmadian, M., Jafari, K.: A Graphene-Based Wide-Band MEMS Accelerometer Sensor Dependent on Wavelength Modulation. IEEE Sens. J. 19, 6226–6232 (2019).
[9]Sani, M.H., Tabrizi, A.A., Saghaei, H., Karimzadeh, R.: An ultrafast all-optical half adder using nonlinear ring resonators in photonic crystal microstructure. Opt. Quantum Electron. 52, 107 (2020).
[10]Parisa Sami, Chao Shen, Mojtaba Hosseinzadeh Sani. Ultra-fast all optical half-adder realized by combining AND/XOR logical gates using a nonlinear nanoring resonator. Applied Optics. Vol. 59, No. 22/1(2020).
[11]B. Liedberg, I. Lundstrom, E. Stenberg, Principles of biosensing with an extended coupling matrix and surface-plasmon resonance, Sens. Actuators B Chem. 11 63–72. (1993).
[12]A. Cavalcanti, B. Shirinzadeh, M. Zhang, and L. C. Retly, “Nanorobot hardware architecture for medical defense,” Sensors, vol. 8, no. 5, pp. 2932- 2958, (2008).
[13]F. Hsiao and C. Lee, “Computational study of photonic crystals nano-ring resonator for biochemical sensing,” IEEE. Sens. J., vol. 10, no. 7, pp. 1185- 1191, (2010).
[14]Blood Glucose monitoring-Wikipedia, the Free Encyclopedia. [Online]. Available: http://en.wikipedia. org/wiki/ Blood_glucose_monitoring, accessed May. 7, (2014).
[15]I. M. White and X. Fan, “On the performance quantification of resonant refractive index sensors,” Opt. Exp., vol. 16, no. 2, pp. 1020–1028, (2008).
[16]D. Jiang, E. Liu, X. Chen, and J. Huang, “Design and properties study of fiber optic glucose biosensor,” Chin. Opt. Lett., vol. 1, no. 2, pp. 108–110, (2003).
[17]A. B. Ganesh and T. K. Radhakrishnan, “Employment of fluorescence quenching for the determination of oxygen and glucose,” Sensors Transducers, vol. 60, no. 10, pp. 439–445, (2005).
[18]Z. Rosenzweig and R. Kopelman, “Analytical properties of miniaturized oxygen and glucose fiber optic sensors,” Sens. Actuators B, Chem., vol. 36, nos. 1–3, pp. 475–483, (1996).
[19]M. Portaccio et al., “Fiber-optic glucose biosensor based on glucose oxidase immobi-lised in a silica gel matrix,” J. Sol-Gel Sci. Technol., vol. 50, no. 3, pp. 437–448, (2009).
[20]M. H. Chiu, S. F. Wand, and R. S. Chang, “D-type fiber biosensor based on surface-plasmon resonance technology and heterodyne interferometry,” Opt. Lett., vol. 30, no. 3, pp. 233–235, (2005).
[21]S.R Joshi et al., “Challenges in diabetes care in India: sheer numbers, lack of awareness and inadequate control,” J. Assoc. Physicians India 56, 443–450. (2008).
[22]Harshita Chopra, Rajinder S. Kaler, Balveer Painam, “Photonic crystal waveguide-based biosensor for detection of diseases” J. Nanophoton., 10(3), 036011. (2016).
[23]Rajendran et al., “Design and Analysis of 2D Photonic Crystal BasedBiosensor to De-tect Different Blood Components” Photonic Sensors / Vol. 9, No. 1, 69–77. (2019).
[24]G. Palai, S.S. Padhee, P. Prakash, P.K. Nayak, Optical characteristics of defect micro-structure fiber using plane wave expansion method, Annual International Conference on Emerging Research Areas and International Conference on Microelectronics, Communications and Renewable Energy, pp. 1–5, (2013).
[25]H. Chopra, R. S. Kaler, and B. Painam. "Photonic crystal waveguide-based biosensor for detection of diseases. "Journal of Nano photonics. (2016).
[26]M. S. Mohamed 1, Mohamed Farhat O. Hameed 2,3, Nihal F. F. Areed 2,4, M. M. El-Okr 5, and S. S. A. Obayya, " Analysis of Highly Sensitive Photonic Crystal Biosensor for Glucose Monitoring. "Aces Journal, Vol. 31, No. 7. (2016).
[27]S. Arafaa, M. Bouchemata, T. Bouchemata, A. Benmerkhi, A. Hocini, "Infiltrated pho-tonic crystal cavity as a highly sensitive platform for glucose concentration detection. "Optics Communications 384 93–100. (2017).
[28]R. Arunkumar, T. Suaganya, And S. Robinson. "Design and Analysis of 2D Photonic Crystal Based Biosensor to Detect Different Blood Components. "Photonic Sensors". (2018).
[29]Almpanis, E, and N. Papanicolaou. "Dielectric nanopatterned surfaces for subwave-length light localization and sensing applications." Microelectronic Engineering 159: 60-632. (2016).
[30]Lu, Xiaoyuan, et al. "Numerical investigation of narrowband infrared absorber and sen-sor based on dielectric-metal metasurface."Optics express" 26.8: 10179-10187.) 2018).